Eyelid Closure in Embryogenesis Is Required for Ocular Adnexa Development

Qinghang Meng,[1] Maureen Mongan,[1] Vinicius Carreira,[1] Hisaka Kurita,[1] Chia-yang Liu,[2] Winston W.-Y. Kao,[2] and Ying Xia[1,2]

[1]Department of Environmental Health, University of Cincinnati, College of Medicine, Cincinnati, Ohio, United States
[2]Ophthalmology, University of Cincinnati, College of Medicine, Cincinnati, Ohio, United States

Correspondence: Ying Xia, Department of Environmental Health, University of Cincinnati, College of Medicine, 123 East Shields Street, Cincinnati, OH 45267-0056, USA; ying.xia@uc.edu.

Submitted: July 3, 2014
Accepted: October 19, 2014

Citation: Meng Q, Mongan M, Carreira V, et al. Eyelid closure in embryogenesis is required for ocular adnexa development. *Invest Ophthalmol Vis Sci*. 2014;55:7652–7661. DOI:10.1167/iovs.14-15155

Purpose. Mammalian eye development requires temporary fusion of the upper and lower eyelids in embryogenesis. Failure of lid closure in mice leads to an eye open at birth (EOB) phenotype. Many genetic mutant strains develop this phenotype and studies of the mutants lead to a better understanding of the signaling mechanisms of morphogenesis. The present study investigates the roles of lid closure in eye development.

Methods. Seven mutant mouse strains were generated by different gene ablation strategies that inactivated distinct signaling pathways. These mice, including systemic ablation of *Map3k1* and *Dkk2,* ocular surface epithelium (OSE) knockout of c-*Jun* and *Egfr*, conditional knockout of *Shp2* in stratified epithelium (SE), as well as the *Map3k1/Jnk1* and *Map3k1/Rhoa* compound mutants, all exhibited defective eyelid closure. The embryonic and postnatal eyes in these mice were characterized by histology and immunohistochemistry.

Results. Some eye abnormalities, such as smaller lens in the *Map3k1*-null mice and Harderian gland hypoplasia in the *Dkk2*-null mice, appeared to be mutant strain–specific, whereas other abnormalities were seen in all mutants examined. The common defects included corneal erosion/ulceration, meibomian gland hypoplasia, truncation of the eyelid tarsal muscles, failure of levator palpebrae superioris (LPS) extension into the upper eyelid and misplacement of the inferior oblique (IO) muscle and inferior rectus (IR) muscle. The muscle defects were traced to the prenatal fetuses.

Conclusions. In addition to providing a protective barrier for the ocular surface, eyelid closure in embryogenesis is required for the development of ocular adnexa, including eyelid and extraocular muscles.

Keywords: embryonic eyelid closure, ocular adnexa, extraocular muscles, tarsal muscles, LPS

Embryonic eyelid closure is a late morphogenetic event fairly well characterized in mice. The mouse eyelid starts to form around embryonic day 11.5 (E11.5) with the invagination of the ocular surface ectoderm adjacent to the eye globe. The epithelium at the eyelid leading edge elongates and migrates centripetally and ultimately fuses between E15.5 and E16.5.[1,2] While the eyelid is closed between E16.5 and postnatal day 12 to 14 in the wild-type mice, it remains widely open in many genetic mutants, leading to an "eye open at birth" (EOB) phenotype.[3] The Mouse Genome Informatics (MGI) has a collection of more than 138 genetic mutant strains displaying the EOB phenotype and the number of mutants is likely to increase with complete or partial knockout of new genes.

The human eyelids also fuse and re-open between 7 and 24 weeks of fetal life. Different from that in mice, however, the human eyelid closure and re-open is accomplished entirely in utero.[4,5] This has made the detection of lid closure defects a major challenge, and as a result, little is truly understood about the incidences of eyelid closure defects and the associated diseases in humans. In this regard, understanding the regulation and function of eyelid closure in mice may help to identify developmental defects associated with lid closure failure in humans.

Over the years, studies of the EOB mutants have significantly advanced our understanding of the signaling mechanisms of tissue morphogenesis. Compelling evidence suggests that eyelid closure requires the RA-RXR/RAR and PITX2-DKK2 pathways and the FOXL2 and OSR2 transcription factors operating in the periocular mesenchyme, as well as the activation of the MAP3K1-JNK, EGFR, ROCK, and PCP pathways in the eyelid epithelial cells.[6–30] In addition, eyelid morphogenesis involves the FGF10-FGFR and BMP-BMPR pathways acting through the mechanisms that involve mesenchymal-epithelium interactions.[3,31] Furthermore, some signaling events are detected in just a few cells within the developing eyelids, indicating that morphogenesis is orchestrated by highly compartmentalized and spatially segregated developmental signals.[16,31,32]

Although the EOB mutant mice are useful tools to investigate the genetic and signaling mechanisms of morphogenesis, little is known about the roles of eyelid closure in eye development. In the present work, we examined several mutant mouse strains and identified common eye defects associated with failure of embryonic eyelid closure. Our data suggest that the closed eyelid protects the ocular surface, as well as serves as a crucial structural support for the development of adnexal structures, including extraocular and

eyelid muscles. Hence, failure of embryonic eyelid closure could be the underlying etiology of or a contributing factor to congenital eye anomalies, such as eyelid ptosis and strabismus.

Materials and Methods

Mice Colonies

The *Map3k1*$^{\Delta/\Delta KD}$, *Map3k1*$^{+/\Delta KD}$/*Jnk1*$^{-/-}$, *Map3k1*$^{+/\Delta KD}$/*Rhoa*$^{\Delta/\Delta OSE}$, and *Le-cre* mice.[15,16,33] the *c-Jun*^{F}, *Dkk2*$^{-/-}$, and *Egfr*^{F} mice[34,35] and the *K14*^{rtTA}/*tet-O-cre/Shp2*$^{F/F}$ mice[36] were as described. The *c-Jun*^{F} and *Egfr*^{F} were crossed with *Le-cre*[37] to generate the *c-Jun*$^{\Delta/\Delta OSE}$ and *Egfr*$^{\Delta/\Delta OSE}$ mice/fetuses. Mice mating and handling and genotyping used standard protocol. All animals were treated in adherence to the ARVO Statement for the Use of Animals in Ophthalmic and Vision Research and procedures were approved by the Institutional Animal Care and Use Committee at the University of Cincinnati (Cincinnati, OH, USA).

Reagents and Antibodies

The antibodies for α-smooth muscle actin (SMA) and keratin 13 (K13) were from Abcam (Cambridge, MA, USA), α-skeletal (SK) myosin and FOXL2 were from Thermal Scientific (Waltham, MA, USA), keratin 10 (K10) and 14 (K14) were from Covance (Princeton, NJ, USA) and Santa Cruz Biotechnology (Dallas, TX, USA), respectively, and keratin 12 (K12) and PITX2 were described before.[38,39] The 4′,6-diamidine-2-phenylindole (DAPI), Harris Hematoxylin solution, and alcoholic Eosin Y solution were from Sigma-Aldrich Corp. (St. Louis, MO, USA), and the Alexa Fluor-conjugated secondary antibodies were from Invitrogen (Carlsbad, CA, USA).

Phenol Red Thread (Schirmer) Test

Mice tear volume was measured by ZONE-QUICK phenol red thread test (Showa YakuhinKako Corp., Chuo-ku, Tokyo, Japan) following manufacturer's instruction. Briefly, mice were anaesthetized by intraperitoneal administration of Avertin at 0.45 mg/g body weight (2, 2, 2-tribromoethanol, Sigma-Aldrich Corp.) and the 3-mm folded region of the thread were inserted into the palpebral conjunctiva of the eye. The thread was removed after 15 seconds, and the tear stained region was measured.

Histology, X-Gal Staining, and Immunostaining

For histology and immunohistochemistry, the embryonic/fetal heads or adult eyes were fixed in 4% paraformaldehyde at 4°C overnight. The tissues were embedded in either optimum cutting temperature (OCT) compound and frozen or paraffin. The entire eye tissues were processed for sagittal sections at 5 or 8 μm. For a complete histologic evaluation, hematoxylin and eosin (H&E) staining was performed on three consecutive sections at every 15 sections throughout the eye, and images were captured using a Zeiss Axioplan 2 imaging fluorescence microscope (Zeiss, Jena, Germany) equipped with AxioVision software. Whole-mount X-gal staining was performed as described previously.[40]

AxioVision software was used to draw lines surrounding the meibomian glands (MG) in each histologic section; the average area and the number of positive sections in each eye were used to calculate the relative size of the MG. Sections within 100 μm of the center of the eye were used for the measurement of lens volume or eyelid length. The lens volume was evaluated by drawing lines surrounding the lens with AxioVision software and using the formula $v = 4/3\pi r^3$. Results represent the average of at least six eyes. The eyelid length was calculated based on the distance between the eyelid tip and the conjunctival fornix of at least four eyes. The H&E stained slides were examined for muscle morphology and representative images were captured using an Axio Scope.A1 (Zeiss) equipped with an AxioCam ERc5s and Zeiss Zen software. The section immediately following the H&E-stained slide was used for immunostaining and at least three eyes or heads were examined per condition.

Statistical Analyses

Statistical comparisons were performed with Student's two-tailed paired *t*-test. Values of $^{*}P < 0.05$, $^{**}P < 0.01$, and $^{***}P < 0.001$ were considered statistically significant.

Results

Eye Defects in *Map3k1*$^{\Delta/\Delta KD}$ and *Dkk2*$^{-/-}$ EOB Mutants at Postnatal Stages

While DKK2 is a regulator of the Wnt pathway, MAP3K1 is a member of the MAP3K family, responsible for signal transduction that leads to the activation of the MAP2K-MAPK cascades.[34,41] Despite that MAP3K1 and DKK2 have distinct signaling properties and developmental roles, the *Map3k1*$^{\Delta/\Delta KD}$ and *Dkk2*$^{-/-}$ mice shared in common the EOB phenotype.[8,15] The anatomic, histologic, and functional features of the mutant eyes and those of their wild-type and heterozygous 6-month-old littermates were summarized in Table 1 (Supplementary Fig. S1A).

Besides the abnormal appearance of the eye, the *Map3k1*$^{\Delta/\Delta KD}$ mice had alterations in the range of microphthalmia with significant smaller lens, in addition to retinal degeneration as we have reported before[42] (Figs. 1A, 1B). Neither the lens nor the retina abnormalities were found in the *Dkk2*$^{-/-}$ mice, suggesting that defective lens and retina development are due to loss of the specific gene functions in the *Map3k1*$^{\Delta/\Delta KD}$ mice.

Both *Map3k1*$^{\Delta/\Delta KD}$ and *Dkk2*$^{-/-}$ mice had significantly reduced tear secretion determined by the Schirmer test (Fig. 1C). The tear film, crucial for keeping the eye moisturized, is produced by the lacrimal and Harderian glands (HG). The HG could be readily identified at the posterior orbit of wild-type, heterozygotes, and *Map3k1*$^{\Delta/\Delta KD}$ mice, but not *Dkk2*$^{-/-}$ mice (Fig. 1D). In the E18.5 fetuses, the compound tubular HG structures detected in the wild type were absent in the *Dkk*$^{-/-}$ fetuses, suggesting that DKK2 is required for HG formation in embryogenesis (Fig. 1E). In contrast, the *Map3k1*$^{\Delta/\Delta KD}$ mice had normal HG, but compared with those in the *Map3k1*$^{+/\Delta KD}$ mice, they had smaller lacrimal glands with more compact lobules (Fig. 1F). Hence, the *Map3k1*-null and *Dkk2*-null mice have distinct gland abnormalities and both result in reduced tear production.

The eyelids of the *Map3k1*$^{\Delta/\Delta KD}$ and *Dkk2*$^{-/-}$ mice had normal size, shape, and length (Supplementary Figs. S1B, S1C) and both had hypoplastic MG with strain-specific features (Fig. 1G). While the *Dkk2*$^{-/-}$ mutants had the glands completely missing in the upper eyelids, the *Map3k1*$^{\Delta/\Delta KD}$ mice had reduced gland sizes in both the upper and lower eyelids (Fig. 1H). The EOB mutants also displayed corneal lesions, and the type and severity of the lesions varied among individuals, suggesting that postnatal or environmental factors contribute, at least partially, to the diverse corneal defects in the EOB mutants (Fig. 1I).

The levator palpebrae superioris (LPS) muscle originates from the back of the globe and is responsible for elevating the upper eyelid. In the wild-type mice, the α-SK myosin–positive

Investigative Ophthalmology & Visual Science

Table 1. Eye Pathology Summary of *Map3k1*$^{\Delta/\Delta KD}$ and *Dkk2*$^{-/-}$ Adults

	Map3k1$^{\Delta/\Delta KD}$	*Dkk2*$^{-/-}$
Eyelid	Eyelid open at birth	Eyelid open at birth
	Chronic blepharitis	Chronic blepharitis
MG	Hypoplastic	Severely hypoplastic
Tarsal muscles	Hypoplastic: shorter, thinner, and truncated	Hypoplastic: shorter, thinner, and truncated
LPS	Shorter and lacking proper insertion into eyelid	Shorter and lacking proper insertion into eyelid
Conjunctiva	Chronic conjunctivitis	Chronic conjunctivitis
	Goblet cell hyperplasia	Goblet cell hyperplasia
		Epithelium Hyperkeratinization (K10 positive)
Cornea	Corneal epithelium hyperplasia	Corneal epithelium hyperplasia
	Corneal epithelium erosion	Corneal epithelium erosion
	Aberrant epithelial differentiation (K12 negative)	Aberrant epithelial differentiation (K12 negative, but K10 positive)
Lens	Volume reduced by 40%	Not different from control
Retina	Folding and degeneration	Not different from control
Optic nerve	Smaller	Normal
Extraocular muscles	More posterior localization of the IR	More posterior localization of the IR
HG	Not different than control	Not present in sections

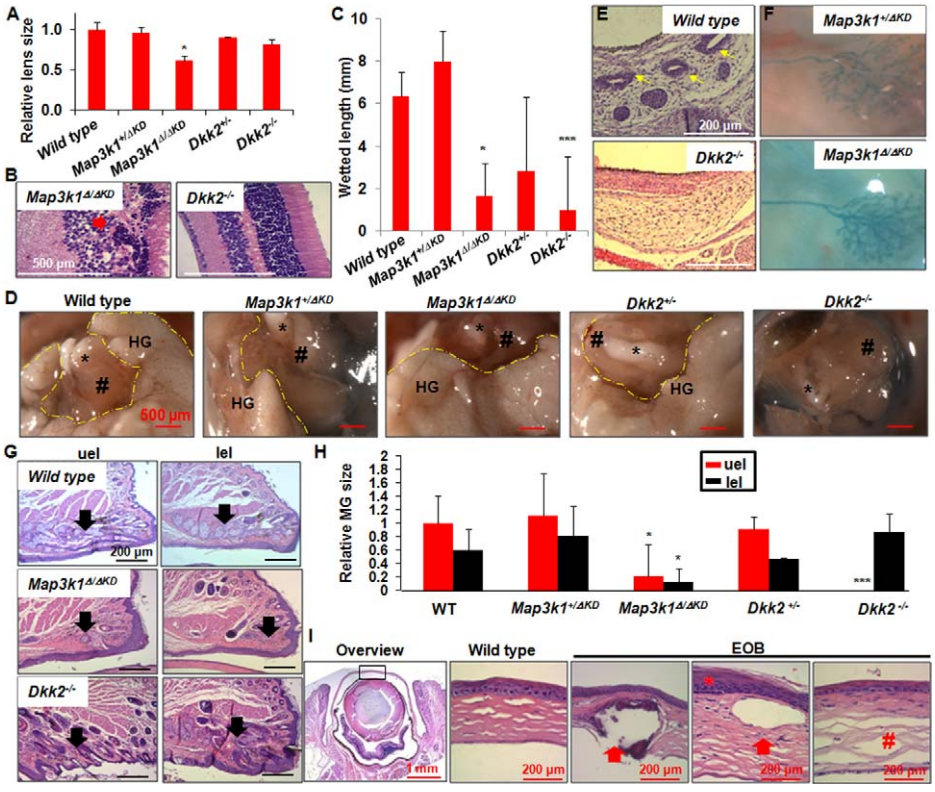

Figure 1. Anatomic, histologic, and functional evaluation of the *Map3k1*$^{\Delta/\Delta KD}$ and *Dkk2*$^{-/-}$ eyes. The 6-month-old wild-type, *Map3k1*$^{+/\Delta KD}$, *Map3k1*$^{\Delta/\Delta KD}$, *Dkk2*$^{+}$, and *Dkk2*$^{-/-}$ mice ($n = 8$) were measured for (**A**) lens size, (**C**) tear volume by Schirmer tests, and (**H**) MG size. (**D**) Photographs of the posterior orbital side of the eyes. The positions of optic nerve (*), extraocular muscle (#), and HG locations were marked (*yellow dotted lines*) (**B**) Histology showed retina dysplasia, characterized by disorganization and decreased cellularity of the inner and outer nuclear layers (*arrow*), in *Map3k1*$^{\Delta/\Delta KD}$, but not *Dkk2*$^{-/-}$ mice. (**E**) Hematoxylin and eosin stained E18.5 wild-type and *Dkk2*$^{-/-}$ eye sections were photographed. The compound tubular structures (*yellow arrows*) of the developing HG were evident in the wild type, but were missing in the *Dkk2*$^{-/-}$ fetuses. (**F**) The E18.5 *Map3k1*$^{+/\Delta KD}$ and *Map3k1*$^{\Delta/\Delta KD}$ fetuses were subjected to whole-mount X-gal staining and the stained lacrimal glands were photographed. (**G**) Hematoxylin and eosin staining of the 6-month-old wild-type, *Map3k1*$^{\Delta/\Delta KD}$, and *Dkk2*$^{-/-}$ eyelids. In the upper (uel) and lower (lel) eyelids, the MG lobules (*black arrows*) were identified in the subepithelial stroma between the conjunctival epithelium and tarsal plate in wild-type mice, but they were inconspicuous in the mutant mice. (**I**) Histologic comparison of the corneas of the 6-month-old wild-type and EOB mice (i.e., *Map3k1*$^{\Delta/\Delta KD}$ and *Dkk2*$^{-/-}$). The EOB corneas displayed dystrophic mineralization, neovascularization, and fibrosis (*red arrows*) with dispersed stroma (#) and epithelium hyperplasia and squamous metaplasia (*). Data analyses were done by the student *t*-test, $^{*}P < 0.05$ and $^{***}P < 0.001$ were considered statistically significant.

Investigative Ophthalmology & Visual Science

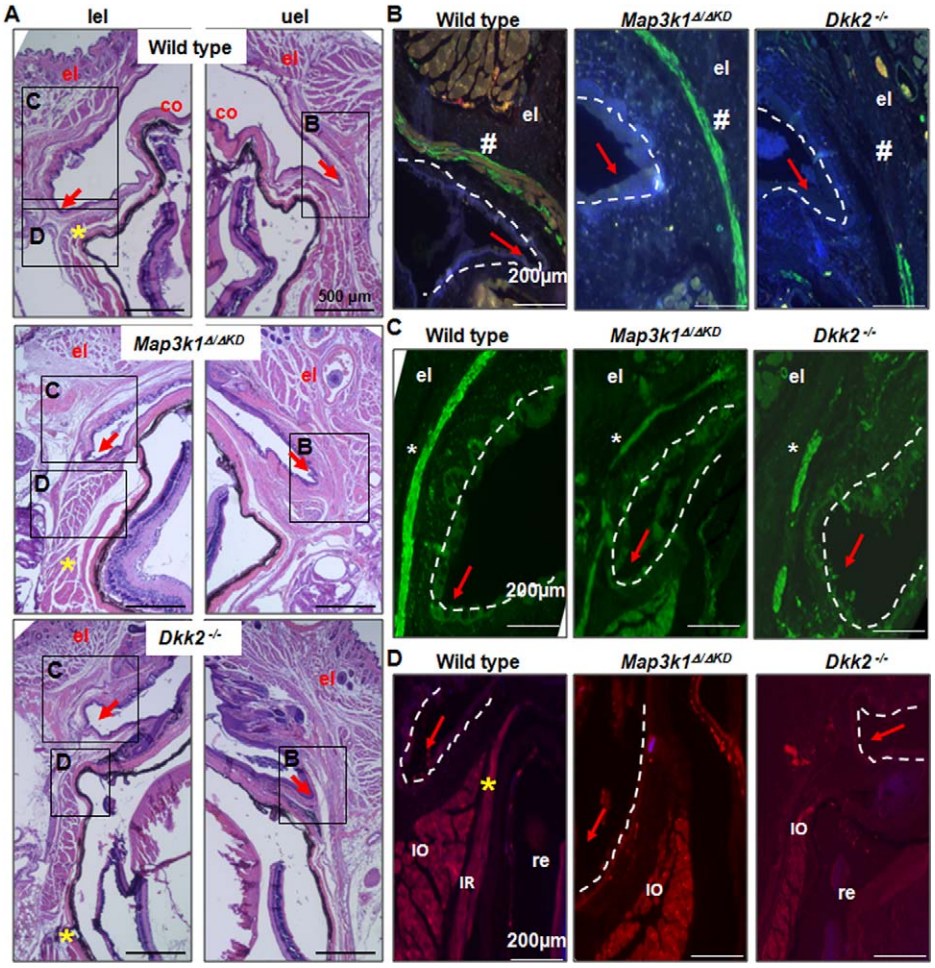

Figure 2. The common eye abnormalities in the *Map3k1*$^{\Delta/\Delta KD}$ and *Dkk2*$^{-/-}$ mice. (**A**) Hematoxylin and eosin and (**B–D**) immunohistochemistry staining of the wild-type, *Map3k1*$^{\Delta/\Delta KD}$, and *Dkk2*$^{-/-}$ eyes in the 6-month-old mice. (**A**) Lower magnification micrograph of the upper (uel) and lower (lel) eyelids. The areas in *rectangle* are shown in higher magnification in (**B–D**) with immunofluorescent staining using anti–α-SMA (*green* in [**B**, **C**]) and anti–α-sk myosin (*red* in [**B**, **D**]). (**B**) In the upper eyelids, the α-sk myosin positive (*red*) LPS (*yellow arrowhead*) extended to and interspersed with the α-SMA–positive (*green*) tarsal muscle (#) in wild type, but were blunt and did not reach to the tarsal muscle in the mutants. In the lower eyelids, (**C**) The eyelid tarsal muscles (*) were continuous in wild type, but truncated in the mutants, (**A**, **D**). The inferior rectus muscle (*yellow asterisks*) inserted at an anterior position on the sclera in the wild type, but at a posterior position in the mutant mice. Pictures were taken using Zeiss microscope Axio Scope A1 or Zeiss Axioplan 2 imaging fluorescence microscope. DAPI (*blue*); el, eyelid; co, cornea; re, retina; IR and *yellow asterisks*; inferior rectus muscle, the *dotted lines*; conjunctival epithelium, and *red arrows*; superior conjunctival fornix.

LPS fully extended through the superior fornix, inserted into the upper eyelid and connected with the tarsal muscles, but in the EOB mice, the LPS failed to extend anteriorly beyond the fornix (Figs. 2A, 2B). The α-SMA–positive tarsal muscles, which act to widen the palpebral fissure and raise the eyelid, extended continuously into the upper and lower eyelid in the wild-type mice, they were short and truncated in the EOB mice (Fig. 2C). The inferior rectus (IR) muscles extended from the back of the globe beyond the fornix, inserted on to the sclera and was overlaid by the inferior oblique (IO) muscle in the wild-type mice, whereas it stopped short before reaching the fornix in the EOB mice (Figs. 2A, 2D). The IR muscles attached to the sclera in the wild-type mice at a position much anterior than that in the EOB mice, as corroborated by the X-ray micro tomography examination, which also detected the abnormal location of IR muscle in the *Map3k1*$^{\Delta/\Delta KD}$ mice, compared with that in the wild-type mice (Supplementary Fig. S1E).

Together, our data show that the *Map3k1*-null and *Dkk2*-null mice exhibit distinct pathologies on lens, retina and orbital glands, a range of abnormalities in cornea and MG, and similar defects in ocular adnexa, including hypoplastic eyelid muscles, and displacement of extraocular muscles.

Eye Defects in Mice Lacking C-Jun and EGFR in Ocular Surface Epithelium

To further identify the eye abnormalities associated with failure of lid closure, we developed two new mutants. The EGFR is a cell surface receptor for many growth factors and cytokines and c-Jun is a transcription factor of the AP-1 family. Both have been shown previously to be essential for promoting the forward movement of the eyelid epithelial cells for embryonic eyelid closure.[43–45] We crossed mice carrying the floxed *c-Jun* or *Egfr* alleles with the *le-cre* mice, which express the Cre recombinase in the ocular surface ectoderm starting on E9.5 and result in ablation of the floxed genes specifically in the

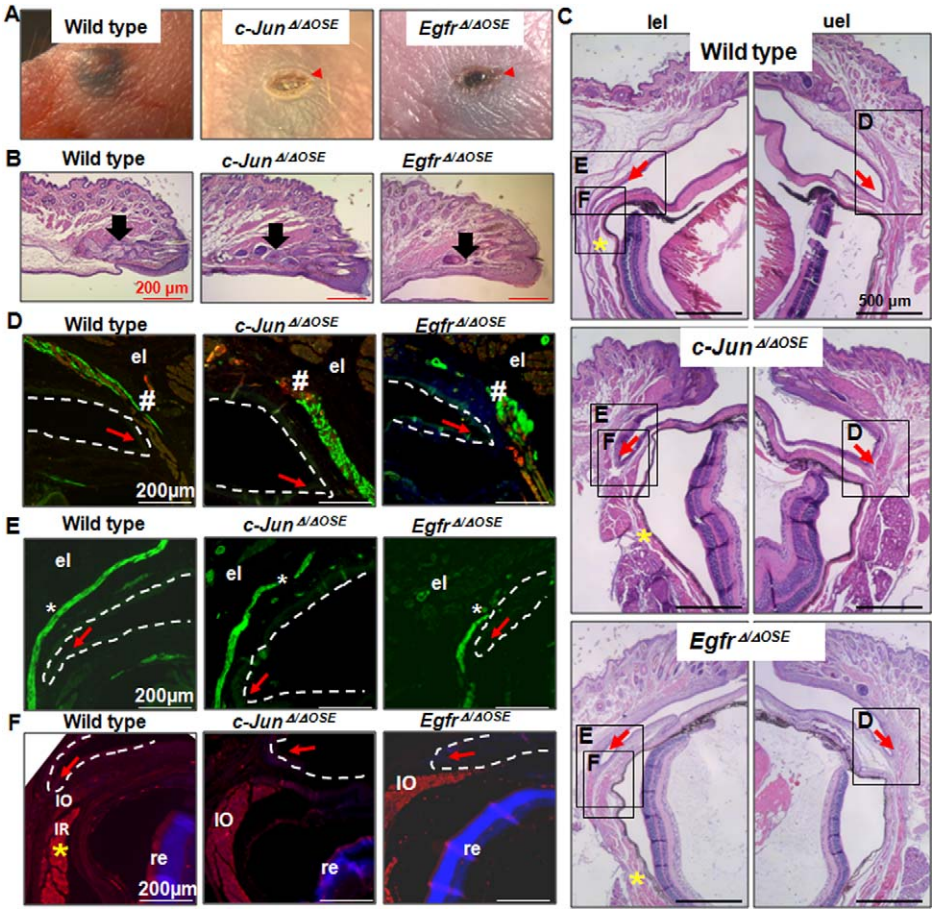

Figure 3. Eye defects in the *c-Jun*$^{\Delta/\Delta OSE}$ and *EGFR*$^{\Delta/\Delta OSE}$ mice. (**A**) The appearance of the wild-type, *c-Jun*$^{\Delta/\Delta OSE}$, and *EGFR*$^{\Delta/\Delta OSE}$ eyes at birth (P1). *Arrowheads* point at the open eyelids in the mutants. At P14, the wild-type, *c-Jun*$^{\Delta/\Delta OSE}$, and *EGFR*$^{\Delta/\Delta OSE}$ eyes were microscopically examined by H&E (**B**, **C**) and immunohistochemistry (**D**–**F**) staining. (**B**) The MG lobules (*black arrows*) were readily identifiable in the wild type but not the mutants. (**C**) Low magnification photomicrographs of the upper (uel) and lower (lel) eyelids. The squared areas are shown in higher magnification in (**D**–**F**) with immunofluorescent staining using anti–α-SMA (*green* in [**D**, **E**]) and anti–α-sk myosin (*red* in [**D**, **F**]). (**D**) In the upper eyelids, the LPS (*red*) extended to and interspersed with the tarsal muscle (#) in wild-type, but misplaced in the mutant upper eyelids. In the lower eyelids, (**E**) the eyelid tarsal muscles (*white asterisks*) were continuous in wild type, but truncated in the mutants, (**C**, **F**) the inferior rectus muscle (*yellow asterisks*) attached to an anterior position on the sclera in the wild type, but to posterior positions in the mutant micethe.

ocular surface epithelium (OSE).[37] When the *c-Jun*$^{\Delta/\Delta OSE}$ and *Egfr*$^{\Delta/\Delta OSE}$ mice were born, approximately 84% and 100% of the offspring, respectively, exhibited the EOB phenotype[46] (Fig. 3A).

Histologic examination of the entire eye showed that, besides corneal damages, the *c-Jun*$^{\Delta/\Delta OSE}$ and *Egfr*$^{\Delta/\Delta OSE}$ mutants had severe hypoplastic MG in both the upper and lower eyelids (Fig. 3B and Supplementary Fig. S1E). Additionally, they exhibited blunted LPS in the upper eyelids (Figs. 3C, 3D), truncated tarsal muscles in the upper and lower eyelids (Figs. 3C, 3E), and misplacement of the IR and IO muscles (Fig. 3C, 3F). Because the genes of interest are ablated specifically in the ocular surface epithelium, the observed muscle phenotype is likely secondary to epithelial cell dysfunction, lending additional support to the notion that failure of eyelid closure associates with abnormal formation and maturation of ocular adnexal structures.

The Fetal Origin of the Ocular Adnexal Phenotypes

The muscle phenotype in the EOB mice could result from genetic mutations that impair muscle growth and differentiation. The development of eyelid tarsal muscle and extraocular muscle commences prior to eyelid closure.[47] In the E15.5 fetuses, we detected the α-SMA–positive tarsal muscle primordia, where FOXL2, a master regulator of muscle differentiation, was also expressed (Fig. 4A). We also identified the phallodin-labeled EOM primordia at the posterior of the eye, where the PITX2, a key regulator of extraocular muscle programming, was detected (Fig. 4B). Importantly, the wild-type and mutant fetuses had similar patterns of tarsal muscle and EOM primordia, and FOXL2 and PITX2 expression, suggesting that the muscle differentiation program was unperturbed by the genetic mutations prior to lid closure.

After eyelid closure, the lid muscles continue to mature and the extraocular muscles insert to sclera. To determine whether the muscle defects could occur after eyelid closure and before birth, we examined the fetuses at E18.5, the embryonic day immediately prior to birth. The anatomic and histologic features of the eyes in the *Map3k1*$^{\Delta/\Delta KD}$, the *Dkk2*$^{-/-}$, and the *c-Jun*$^{\Delta/\Delta OSE}$ fetuses and their wild-type and heterozygous littermates were summarized in Table 2. In contrast to the wild-type fetuses having eyelid tarsal muscles extended continuously into the upper and lower eyelids, the mutant fetuses with defective eyelid closure had truncated eyelid tarsal muscles (Figs. 5A, 5B). The IO muscle, expressing both α-SMA and α-sk-myosin, extended anteriorly and stopped before reaching the

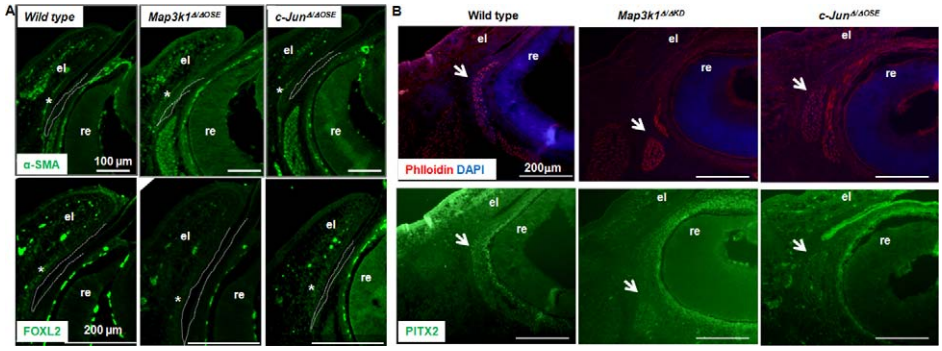

Figure 4. Muscle differentiation unaffected in the mutant fetuses prior to lid closure. The E15.5 fetuses were subjected to immunostaining using (**A**) anti-α-SMA (*upper panels*) and anti-FOXL2 (*lower panels*). The tarsal muscles were labeled with *asterisks* and *dotted lines* marked the conjunctival epithelium, and (**B**) phallodin and DAPI (*upper panels*) and anti-PITX2 (*lower panels*). The extraocular muscle primordia were indicated (*white arrows*).

level of the superior conjunctival fornix in the wild-type fetuses, yet, in all the mutant fetuses, they extended further and inserted at a location past the fornix level.

If the muscle phenotype were linked to defective eyelid closure, they should occur in other lid closure defective strains. The SHP2 is a protein tyrosine phosphatase known to modulate the EGFR signaling pathway. We crossed the *Shp2* floxed mice with the *K14-rtTA/tet-o-Cre* mice. Administration of doxycycline at E14.5 ablated the *Shp2* gene in stratified epithelial (SE) keratinocytes, including epidermis, cornea and conjunctiva, in the compound mutant fetuses ($Shp2^{\Delta/\Delta SE}$) and resulted in an EOB phenotype (Fig. 5C). We previously crossed the $Map3k1^{\Delta KD}$ with the *Jnk1*- and $Rhoa^{\Delta OSE}$-mutant mice and showed that the $Map3k1^{+/\Delta KD}Jnk1^{-/-}$ compound mutant mice had their eyelids widely open at birth, but the $Map3k1^{+/\Delta KD}/Rhoa^{\Delta/\Delta OSE}$ fetuses had delayed eyelid closure.[14,33] The eyelids of the $Map3k1^{+/\Delta KD}/Rhoa^{\Delta/\Delta OSE}$ fetuses were still partially open at E17.5, but closed at E18.5. While all the mutant strains displayed truncated tarsal muscle and misplacement of IO muscle, the phenotypes were more pronounced in the $Map3k1^{+/\Delta KD}/Jnk1^{-/-}$ and $Shp2^{\Delta/\Delta SE}$ fetuses, and less obvious in the $Map3k1^{+/\Delta KD}/Rhoa^{\Delta/\Delta OSE}$ fetuses (Fig. 4D). Thus, all the mutants display muscle insertion abnormalities, and furthermore, the severity of the muscle phenotype correlates to the magnitude of eyelid closure failure.

By measuring the distance between muscle-sclera insertion and conjunctival fornix, we showed that the IO muscle inserted to sclera either lateral or posterior to the conjunctival fornix in the wild-type fetuses; however, it was extended beyond the conjunctival fornix and inserted into the sclera approximately 200-μm anterior to the fornix in all the mutants with failure of eyelid closure (Fig. 4E). Our data suggest that although the genetic mutations do not impair eyelid and extraocular muscle differentiation, they cause defective eyelid closure, which may in turn impose physiological restraint on muscle development and site of insertion to sclera in the prenatal fetuses.

Eyelid Closure Is Dispensable for the Prenatal Cornea and Conjunctiva Development

The corneal development commences between E11 and E12 and completes at postnatal day 12 and 14.[48] It is proposed that closure of the eyelids results in the formation of the conjunctiva sac that is required for corneal maturation. However, in the E18.5 fetuses, all mutants had normal corneal morphology and K12 and K14 expression in the epithelial layer regardless of the genotype and eyelid closure status (Figs. 6A, 6B). Consistent with the notion that DKK2 is required for the corneal epithelial cell fate, the $Dkk2^{-/-}$ mutants expressed the skin differentiation marker K10 in the corneal epithelium, as well as detectable hair follicle germ and peg[49] (Figs. 5C, 5D). None of the other mutants had K10 expression in the corneal epithelium.

Table 2. Eye Pathology of $Map3k1^{\Delta/\Delta KD}$, $Dkk2^{-/-}$, and $Jun^{\Delta/\Delta OSE}$ E18.5 Embryos

	$Map3k1^{\Delta/\Delta KD}$	$Dkk2^{-/-}$	$Jun^{\Delta/\Delta OSE}$
Eyelid	Eyelid open	Eyelid open; shorter upper eyelid	Eyelid open
MG	Undetectable	Undetectable	Undetectable
	Not different from control	Not different from control	Not different from control
Tarsal muscles	Shorter and truncated	Shorter and truncated	Shorter and truncated
LPS	Not different than control	Not different than control	Not different than control
Conjunctiva	Not different than control	Squamous metaplasia of the conjunctiva epithelium, and K10 positive;	Not different than control
Cornea	Corneal epithelium hyperplasia	Corneal epithelium hyperplasia Squamous metaplasia of the corneal epithelium, K10 positive, hair follicle positive	Thinner stroma
Lens	Approximately 30% Smaller	Not different than control	Approximately 50% smaller
Retina	Not different than control	Not different than control	Not different than control
Optic nerve	Not different than control	Not different than control	Not different than control
Extraocular muscles	Aberrant IO insertion in sclera	Aberrant IO insertion in sclera	Aberrant IO insertion in sclera
HG	Not different than control	Not present in sections	Not different than control

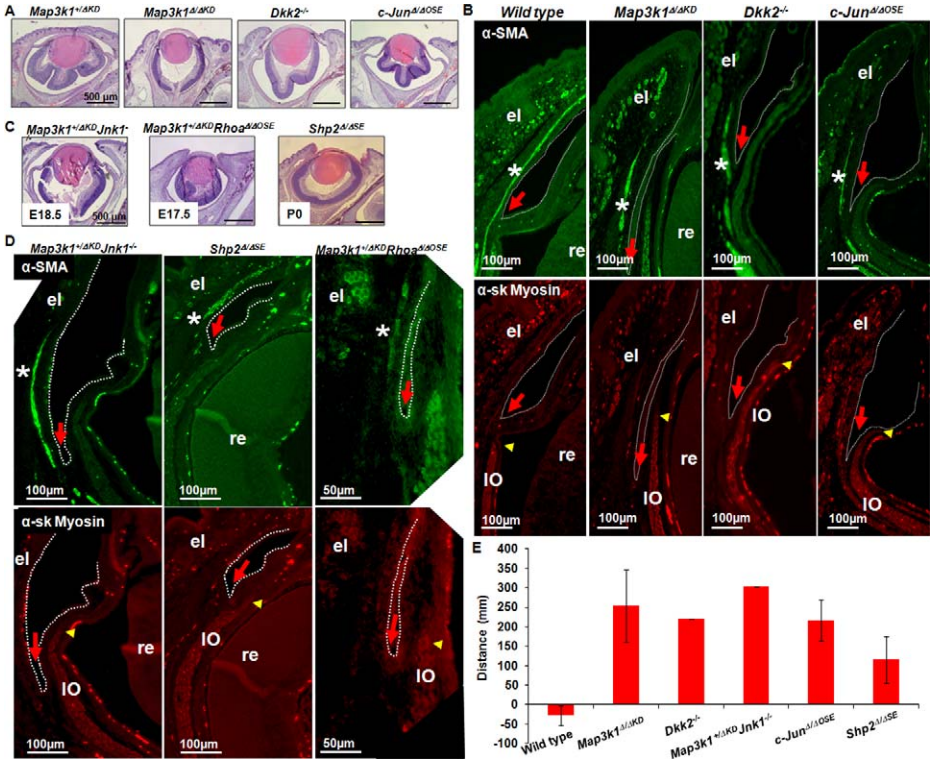

Figure 5. Defective eyelid muscle corresponds to failure of eyelid closure in the E18.5 fetuses. The sagittal eye sections of (**A**, **B**) the E18.5 wild-type, *Map3k1*$^{\Delta/\Delta KD}$, *Dkk2*$^{-/-}$, and *c-Jun*$^{\Delta/\Delta OSE}$ fetuses, and (**C**, **D**) the E17.5 – P0 *Map3k1*$^{+/\Delta KD}$*Jnk1*$^{-/-}$, *Map3k1*$^{+/\Delta KD}$, *Rhoa*$^{\Delta/\Delta OSE}$, and *Shp2*$^{\Delta/\Delta SE}$ mutants were examined by H&E (**A**, **C**) and immunohistochemistry staining (**B**, **D**) using anti–α-SMA (*green*) and anti–α-sk myosin (*red*) to examine the eyelid and extraocular muscles. (**A**, **C**) The wild-type eyelids were fused, but all the mutants' eyelids were open, and (**B**, **D**) the tarsal muscles (*asterisks*) are continuous in the wild type, but truncated in the mutant fetuses; the IO muscles (*yellow arrowheads*) were located posterior to the conjunctival fornix (*red arrows*) in the wild-type, but extended beyond the fornix in the mutant fetuses. (**E**) The distance between IO muscle tip (*yellow arrowheads*) and conjunctival fornix (*red arrows* in [**B**] and [**D**]) was measured ($n = 3$) using AxioVision software. While the IO muscles in the wild-type fetuses were slightly posterior to the fornix, those in the mutant fetuses extended 100- to 200-μm anteriorly beyond the fornix. *Asterisk* indicates tarsal muscle.

The MG anlages were still indiscernible in the E18.5 fetuses, when the dense MG placodes just start to form in between the fused lid junction.[50] We asked whether eyelid closure was required for differentiation of the conjunctival epithelium that gave rise to the MG. At E18.5, the expression of K13, a marker of conjunctival epithelium, was abolished in the upper eyelids of the *Dkk2*$^{-/-}$, but detected in the *Map3k1*$^{\Delta/\Delta KD}$ and *c-Jun*$^{\Delta/\Delta OSE}$ similar to that in wild-type and *Map3k1*$^{+/\Delta KD}$ fetuses (Fig. 6E). At PD1, K13 expression was markedly reduced in the *Map3k1*$^{\Delta/\Delta KD}$ and *c-Jun*$^{\Delta/\Delta OSE}$ mice (Fig. 6F).

Collectively, the data presented here show that closure of the eyelid is dispensable, but DKK2 is required, for corneal and conjunctival epithelial differentiation in the prenatal fetuses; however, a closed eyelid offers protection for the corneal and conjunctival epithelium after birth.

Discussion

Embryonic eyelid fusion is an essential morphogenetic event in mammals. After the lid closure, the cornea becomes mature and the ocular auxiliary tissues, including the tarsal plate, a fibrous layer that gives the lids shape, strength, and a place for muscles to attach, and the MG, lying underneath and within the tarsal plate, producing meibum that prevents evaporation of the tear film, start to form. Although the roles of lid closure are still poorly understood, it is reasonable to speculate that it is required for development of some of these eye structures. By examining seven mutant mouse strains with defective embryonic eyelid closure, we show that in addition to providing a physical barrier, the closed eyelid offers structural support for the formation of ocular adnexal structures, including eyelid and extraocular muscles (Fig. 7). The adult mice with eyelid closure failure display eyelid tarsal muscle hypoplasia, blunted LPS extension and misplaced IR muscles. In the E18.5 fetuses, defective eyelid closure is associated with truncated tarsal muscles and misplacement of IO muscles.

The eyelid tarsal muscle defects can result from downregulation of FOXL2 in the neural crest–derived periocular mesenchymal cells, leading to impaired muscle differentiation.[51] The extraocular muscle abnormality occurs in the mesoderm-specific *Pitx2* knockout embryos where PITX2 is required for myosin expression and myogenic differentiation.[52] None of these mechanisms, however, are responsible for the muscle abnormalities in the EOB mutants studied here. We have shown that the muscle differentiation and expression of FOXL2 and PITX2 are unperturbed in the mutant embryos. Some of the genes are inactivated specifically in the ocular surface epithelial cells, raising the possibility that the muscle defects in the mutants are secondary to epithelial dysfunctions. Moreover, the muscle abnormalities are detectable only at the late fetal stages, suggesting that they are likely the consequences of failure of eyelid closure. Our data support the idea that eyelid closure provides morphological scaffold for the development of adnexal structures, including extension of eyelid tarsal muscle and LPS, and sclera insertion of the extraocular muscle and that congenital abnormalities affecting

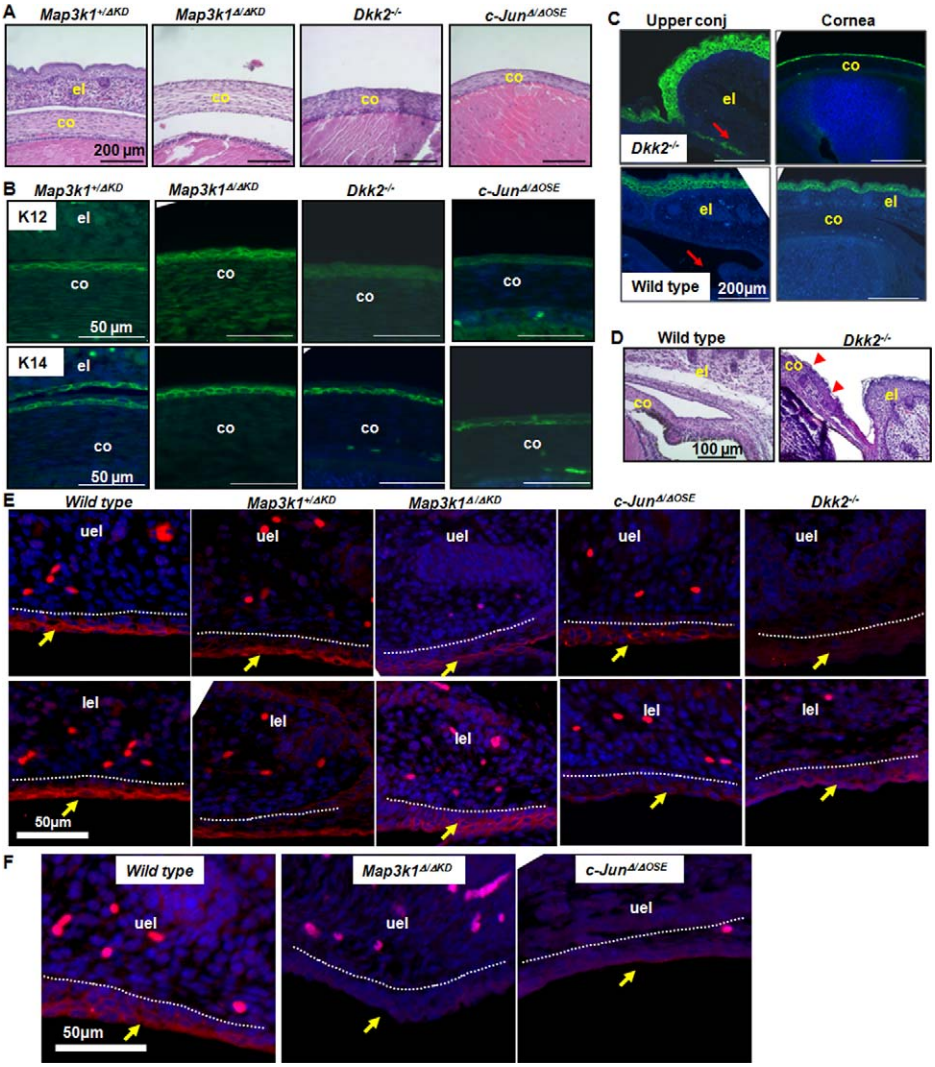

Figure 6. Characterization of the cornea and conjunctiva in wild-type and mutant mice. The wild-type, *Map3k1*$^{\Delta/\Delta KD}$, *Dkk2*$^{-/-}$, and *c-Jun*$^{\Delta/\Delta OSE}$ eyes were examined by H&E staining (**A**, **D**), and immunofluorescence staining (**B**, **C**, **E**, **F**). (**A**) Histologic examination showed that all E18.5 fetuses had comparable corneal morphology, and (**B**) with the normal expression (*green*) of K12 and K14 in the corneal epithelial cells. (**C**) Although keratin 10 (*green*) was not expressed in the corneal or conjunctival epithelium of the wild-type fetuses, it was expressed in those of the *Dkk2*$^{-/-}$ fetuses. (**D**) The hair follicle germ and peg (*arrowheads*) in the cornea of *Dkk2*$^{-/-}$ fetuses. Immunofluorescence staining detected K13 expression (**E**) in the conjunctival epithelium (*yellow arrows*) of the E18.5 wild-type, *Map3k1*$^{+/\Delta KD}$, *Map3k1*$^{\Delta/\Delta KD}$, and *c-Jun*$^{\Delta/\Delta OSE}$ fetuses and lower, but not upper, eyelids of the *Dkk2*$^{-/-}$ fetuses, and (**F**) in the conjunctival epithelium of the postnatal day 1 (PD1) wild-type, but not *Map3k1*$^{\Delta/\Delta KD}$ and *c-Jun*$^{\Delta/\Delta OSE}$ mice. *Red arrows* indicate superior conjunctival fornix.

these ocular adnexa structures may have defective eyelid closure as one of the underlying causes.

All the EOB mice exhibit corneal dystrophy and MG hypoplasia, but the causes of these phenotypes appear to be complex. One possible contributing factor is the genetic mutations that impair differentiation. In the *Dkk2*$^{-/-}$ mutants, we detect the co-expression of K10 with K13 in conjunctiva and co-expression of K10 with K12 in cornea, suggesting that the cell lineages are diverged from the conventional epithelium. The *Dkk2*$^{-/-}$ mutants display aberrant conjunctiva epithelium differentiation in prenatal fetuses and hypoplastic MG in adults, both defects are more pronounced in the upper eyelids. Another possible contributing factor is the environmental insults.[53] The *Map3k1*$^{\Delta/\Delta KD}$ and c-Jun$^{\Delta/\Delta OSE}$ mice have normal K13 expression in the prenatal fetuses, but markedly reduced expression after birth, corresponding to hypoplastic MG in adult mice. Similarly, all the EOB mice display exposure-driven remodeling changes of the cornea, including corneal epithelial erosion, hyperplasia, and squamous metaplasia as well as corneal stroma neovascularization. The corneal lesions are absent in the prenatal fetuses. The fact that many of the corneal and conjunctival abnormalities are detected only in the postnatal EOB mice suggests that the combination of premature exposure and the unfavorable postnatal environment is the etiology. The closed eyelid in this context is a physical barrier protecting the cornea and conjunctiva in neonatal mice from environmental insults.

One of the goals of our work is to translate the molecular findings in mice to an understanding relevant to the genesis of ocular birth defects in humans. The morphogenetic process of the eyelid closure in humans is parallel to the one in mice, and so is the development of adnexal structures. During the time when the human eyelid is closed, the orbicularis oculi muscle and tarsal plate become mature, the smooth muscles attach to the tarsal plate responsible for eyelid elevation.[31,32,54] In light of the findings in mice, eyelid closure in humans may also be

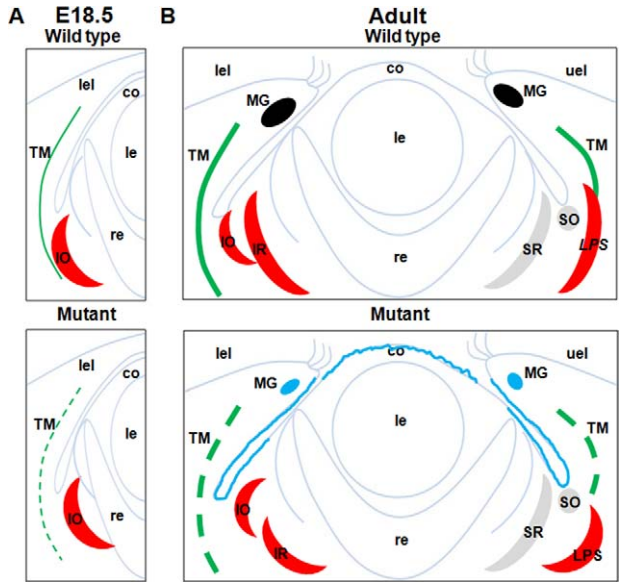

Figure 7. The developmental roles of embryonic eyelid closure. (**A**) Failure of eyelid closure in embryogenesis causes truncated tarsal muscles and misplacement (anterior extension) of the IO muscle in fetal development, and it leads to the adult phenotype in (**B**), including truncated tarsal muscles, blunted LPS, abnormal sclera insertion site of the *IR* muscles. After birth, the EOB mice may develop exposure-driven remodeling changes (*bright blue*) of cornea, conjunctiva and MG. TM, tarsal muscle; SO, superior oblique.

crucial for tarsal muscles development, LPS extension and extraocular muscle proper insertion; conversely, failure of eyelid closure may lead to congenital diseases, such as blepharoptosis.

On the other hand, the closed eyelids in humans separate merely the cornea from the amniotic fluid, thus, many of the protective roles of eyelid closure against exposure-driven remodeling changes in the cornea and MG observed in mice might not apply to humans.[31,32] Sevel[31] has noted that the human fetal renal function commences coinciding with the completion of eyelid closure, and he proposes that the closed eyelid separates the immature eye from the renal excretions, protecting the eye from damages by urea, uric acid, and creatinine. Along the line of this idea, the closed eyelids may protect the eyes from harmful environmental insults that the mothers may be exposed to at the early stages of pregnancy. Failure of eyelid closure is, therefore, likely to be one of the underlying causes of maternal exposure-induced congenital ocular surface anomalies, such as corneal clouding and dystrophies, lens cataract, and coloboma.[32]

As the "risk factors" for EOB in mice have rapidly expanded to hundreds of genetic mutations, as well as multifactorial causes involving gene–gene and gene–environment interactions, the information derived from mice may guide the future development of imaging and genetic studies in the human patients.[14,29,33] This may ultimately lead to the identification of the eyelid closure defect as an etiologic agent of a subset of human birth defects.

Acknowledgments

The authors thank Randall Johnson (University of California, San Diego, CA, USA), Dianqing Wu (Yale University, New Haven, CT, USA), David Threadgill for providing genetically manipulated mice, Tord Hjalt (Lund University, Scania, Sweden) and Philip Gage (University of Michigan, Ann Arbor, MI, USA) for the PITX2 antibody, and Diana Lindquist and John Pearce (Cincinnati Children's Hospital, Cincinnati, OH, USA) for performing micro-CT.

Supported by a National Institutes of Health Grants EY15227 (YX; Bethesda, MD, USA).

Disclosure: **Q. Meng**, None; **M. Mongan**, None; **V. Carreira**, None; **H. Kurita**, None; **C.-Y. Liu**, None; **W.W.-Y. Kao**, None; **Y. Xia**, None

References

1. Findlater GS, McDougall RD, Kaufman MH. Eyelid development, fusion and subsequent reopening in the mouse. *J Anat*. 1993;183:121–129.
2. Harris MJ, McLeod MJ. Eyelid growth and fusion in fetal mice. A scanning electron microscope study. *Anat Embryol (Berl)*. 1982;164:207–220.
3. Tao H, Ono K, Kurose H, Noji S, Ohuchi H. Exogenous FGF10 can rescue an eye-open at birth phenotype of Fgf10-null mice by activating activin and TGFalpha-EGFR signaling. *Dev Growth Differ*. 2006;48:339–346.
4. Matt N, Dupe V, Garnier JM, et al. Retinoic acid-dependent eye morphogenesis is orchestrated by neural crest cells. *Development*. 2005;132:4789–4800.
5. Molotkov A, Molotkova N, Duester G. Retinoic acid guides eye morphogenetic movements via paracrine signaling but is unnecessary for retinal dorsoventral patterning. *Development*. 2006;133:1901–1910.
6. Gage PJ, Qian M, Wu D, Rosenberg KI. The canonical Wnt signaling antagonist DKK2 is an essential effector of PITX2 function during normal eye development. *Dev Biol*. 2008;317:310–324.
7. Schaeper U, Vogel R, Chmielowiec J, Huelsken J, Rosario M, Birchmeier W. Distinct requirements for Gab1 in Met and EGF receptor signaling in vivo. *Proc Natl Acad Sci U S A*. 2007;104:15376–15381.
8. Qu CK, Yu WM, Azzarelli B, Feng GS. Genetic evidence that Shp-2 tyrosine phosphatase is a signal enhancer of the epidermal growth factor receptor in mammals. *Proc Natl Acad Sci U S A*. 1999;96:8528–33.
9. Crotty T, Cai J, Sakane F, Taketomi A, Prescott SM, Topham MK. Diacylglycerol kinase delta regulates protein kinase C and epidermal growth factor receptor signaling. *Proc Natl Acad Sci U S A*. 2006;103:15485–15490.
10. Wojnowski L, Stancato LF, Zimmer AM, et al. Craf-1 protein kinase is essential for mouse development. *Mech Dev*. 1998;76:141–149.
11. Scholl FA, Dumesic PA, Barragan DI, et al. Mek1/2 MAPK kinases are essential for Mammalian development, homeostasis, and Raf-induced hyperplasia. *Dev Cell*. 2007;12:615–629.
12. Schwartzberg PL, Stall AM, Hardin JD, et al. Mice homozygous for the ablm1 mutation show poor viability and depletion of selected B and T cell populations. *Cell*. 1991;65:1165–1175.
13. Zhang L, Wang W, Hayashi Y, et al. A role for MEK kinase 1 in TGF-beta/activin-induced epithelium movement and embryonic eyelid closure. *Embo J*. 2003;22:4443–4454.
14. Takatori A, Geh E, Chen L, Zhang L, Meller J, Xia Y. Differential transmission of MEKK1 morphogenetic signals by JNK1 and JNK2. *Development*. 2008;135:23–32.
15. Weston CR, Wong A, Hall JP, Goad ME, Flavell RA, Davis RJ. JNK initiates a cytokine cascade that causes Pax2 expression and closure of the optic fissure. *Genes Dev*. 2003;17:1271–1280.
16. Schramek D, Kotsinas A, Meixner A, et al. The stress kinase MKK7 couples oncogenic stress to p53 stability and tumor suppression. *Nat Genet*. 2011;43:212–219.
17. Thumkeo D, Shimizu Y, Sakamoto S, Yamada S, Narumiya S. ROCK-I and ROCK-II cooperatively regulate closure of eyelid

and ventral body wall in mouse embryo. *Genes Cells*. 2005;10: 825–834.

18. Rice DS, Hansen GM, Liu F, et al. Keratinocyte migration in the developing eyelid requires LIMK2. *PLoS One*. 2012;7:e47168.
19. Shimizu Y, Thumkeo D, Keel J, et al. ROCK-I regulates closure of the eyelids and ventral body wall by inducing assembly of actomyosin bundles. *J Cell Biol*. 2005;168:941–953.
20. Kibar Z, Vogan KJ, Groulx N, Justice MJ, Underhill DA, Gros P. LTAP, a mammalian homolog of Drosophila Strabismus/Van Gogh, is altered in the mouse neural tube mutant Loop-tail. *Nat Genet*. 2001;28:251–255.
21. Murdoch JN, Doudney K, Paternotte C, Copp AJ, Stanier P. Severe neural tube defects in the loop-tail mouse result from mutation of Lpp1, a novel gene involved in floor plate specification. *Hum Mol Genet*. 2001;10:2593–2601.
22. Hamblet NS, Lijam N, Ruiz-Lozano P, et al. Dishevelled 2 is essential for cardiac outflow tract development, somite segmentation and neural tube closure. *Development*. 2002; 129:5827–5838.
23. Curtin JA, Quint E, Tsipouri V, et al. Mutation of Celsr1 disrupts planar polarity of inner ear hair cells and causes severe neural tube defects in the mouse. *Curr Biol*. 2003;13: 1129–1133.
24. Lu X, Borchers AG, Jolicoeur C, Rayburn H, Baker JC, Tessier-Lavigne M. PTK7/CCK-4 is a novel regulator of planar cell polarity in vertebrates. *Nature*. 2004;430:93–98.
25. Montcouquiol M, Rachel RA, Lanford PJ, Copeland NG, Jenkins NA, Kelley MW. Identification of Vangl2 and Scrb1 as planar polarity genes in mammals. *Nature*. 2003;423:173–177.
26. Harris MJ, Juriloff DM. Mouse mutants with neural tube closure defects and their role in understanding human neural tube defects. *Birth Defects Res A Clin Mol Teratol*. 2007;79: 187–210.
27. Rivera C, Simonson SJ, Yamben IF, et al. Requirement for Dlgh-1 in planar cell polarity and skeletogenesis during vertebrate development. *PLoS One*. 2013;8:e54410.
28. Torban E, Patenaude AM, Leclerc S, et al. Genetic interaction between members of the Vangl family causes neural tube defects in mice. *Proc Natl Acad Sci U S A*. 2008;105:3449–3454.
29. Huang J, Dattilo LK, Rajagopal R, et al. FGF-regulated BMP signaling is required for eyelid closure and to specify conjunctival epithelial cell fate. *Development*. 2009;136: 1741–1750.
30. Wu CI, Hoffman JA, Shy BR, et al. Function of Wnt/beta-catenin in counteracting Tcf3 repression through the Tcf3-beta-catenin interaction. *Development*. 2012;139:2118–2129.
31. Sevel D. A reappraisal of the development of the eyelids. *Eye*. 1988;2:123–129.
32. Byun TH, Kim JT, Park HW, Kim WK. Timetable for upper eyelid development in staged human embryos and fetuses. *Anat Rec (Hoboken)*. 2011;294:789–796.
33. Geh E, Meng Q, Mongan M, et al. Mitogen-activated protein kinase kinase kinase 1 (MAP3K1) integrates developmental signals for eyelid closure. *Proc Natl Acad Sci U S A*. 2011;108: 17349–17354.
34. Li X, Liu P, Liu W, et al. Dkk2 has a role in terminal osteoblast differentiation and mineralized matrix formation. *Nat Genet*. 2005;37:945–952.
35. Maklad A, Nicolai JR, Bichsel KJ, et al. The EGFR is required for proper innervation to the skin. *J Invest Dermatol*. 2009;129: 690–698.
36. Ng GY, Yeh LK, Zhang Y, et al. Role of SH2-containing tyrosine phosphatase Shp2 in mouse corneal epithelial stratification. *Invest Ophthalmol Vis Sci*. 2013;54:7933–7942.
37. Ashery-Padan R Marquardt T Zhou X Gruss P. Pax6 activity in the lens primordium is required for lens formation and for correct placement of a single retina in the eye. *Genes Dev*. 2000;14:2701–2711.
38. Liu CY, Zhu G, Westerhausen-Larson A, et al. Cornea-specific expression of K12 keratin during mouse development. *Curr Eye Res*. 1993;12:963–974.
39. Hjalt TA, Semina EV, Amendt BA, Murray JC. The Pitx2 protein in mouse development. *Dev Dyn*. 2000;218:195–200.
40. Mongan M, Tan Z, Chen L, et al. Mitogen-activated protein kinase kinase kinase 1 protects against nickel-induced acute lung injury. *Toxicol Sci*. 2008;104:405–411.
41. Craig EA, Stevens MV, Vaillancourt RR, Camenisch TD. MAP3Ks as central regulators of cell fate during development. *Dev Dyn*. 2008;237:3102–3114.
42. Mongan M, Wang J, Liu H, et al. Loss of MAP3K1 enhances proliferation and apoptosis during retinal development. *Development*. 2011;138:4001–4012.
43. Zenz R, Scheuch H, Martin P, et al. c-Jun regulates eyelid closure and skin tumor development through EGFR signaling. *Dev Cell*. 2003;4:879–889.
44. Sibilia M, Steinbach JP, Stingl L, Aguzzi A, Wagner EF. A strain-independent postnatal neurodegeneration in mice lacking the EGF receptor. *Embo J*. 1998;17:719–731.
45. Luetteke NC, Qiu TH, Fenton SE, et al. Targeted inactivation of the EGF and amphiregulin genes reveals distinct roles for EGF receptor ligands in mouse mammary gland development. *Development*. 1999;126:2739–2750.
46. Meng Q, Mongan M, Wang J, et al. Epithelial sheet movement requires the cooperation of c-Jun and MAP3K1. *Dev Biol*. 2014;395:29–37.
47. Porter JD, Baker RS. Prenatal morphogenesis of primate extraocular muscle: neuromuscular junction formation and fiber type differentiation. *Invest Ophthalmol Vis Sci*. 1992;33: 657–670.
48. Zieske JD. Corneal development associated with eyelid opening. *Int J Dev Biol*. 2004;48:903–911.
49. Mukhopadhyay M, Gorivodsky M, Shtrom S, et al. Dkk2 plays an essential role in the corneal fate of the ocular surface epithelium. *Development*. 2006;133:2149–2154.
50. Nien CJ, Massei S, Lin G, et al. The development of meibomian glands in mice. *Mol Vis*. 2010;16:1132–1140.
51. Zhang Y, Kao WW, Pelosi E, Schlessinger D, Liu CY. Notch gain of function in mouse periocular mesenchyme downregulates FoxL2 and impairs eyelid levator muscle formation, leading to congenital blepharophimosis. *J Cell Sci*. 2011;124:2561–2572.
52. Zacharias AL, Lewandoski M, Rudnicki MA, Gage PJ. Pitx2 is an upstream activator of extraocular myogenesis and survival. *Dev Biol*. 2011;349:395–405.
53. Suhalim JL, Parfitt GJ, Xie Y, et al. Effect of desiccating stress on mouse meibomian gland function. *Ocul Surf*. 2014;12:59–68.
54. Doxanas MT, Anderson RL. Oriental eyelids. An anatomic study. *Arch Ophthalmol*. 1984;102:1232–1235.

Investigative Ophthalmology & Visual Science